

ELECTRONIC SUPPLEMENTARY INFORMATION

Dielectrophoretic trapping of nanosized biomolecules on plasmonic nanohole arrays for biosensor applications: Simple fabrication and visible-region detection

Satoko Fujiwara,^a Misaki Hata,^b Ikumi Onohara,^b Daiki Kawasaki,^a Kenji Sueyoshi,^{a,c} Hideaki Hisamoto,^a Masato Suzuki,^b Tomoyuki Yasukawa^b and Tatsuro Endo^{*a}

^aDepartment of Applied Chemistry, Graduate School of Engineering, Osaka Metropolitan University, 1-1 Gakuen-cho, Naka-ku, Sakai, Osaka 599-8531, Japan.

^bGraduate School of Material Science, University of Hyogo, 3-2-1 Kouto, Kamigori, Ako, Hyogo 678-1297, Japan.

^cJapan Science and Technology Agency (JST), Precursory Research for Embryonic Science and Technology (PRESTO) 4-1-8 Honcho, Kawaguchi, Saitama 332-0012, Japan.

^dAdvanced Medical Engineering Research Institute, University of Hyogo, Hyogo, Japan.

* Corresponding author: Tatsuro Endo (t_endo@omu.ac.jp)

Fig. S1: (a) Schematic of the optical setup used to measure the transmission spectra. (b) and (c) Overview images of the FDTD simulation model of the Au NHA.

Fig. S2: (a) Transmission spectra with respect to an *RI* change and EM fields of the Au NHA. (b) Peak and dip shifts with respect to the *RI* at 776 and 788 nm simulated using the FDTD method. □

Fig. S3: ES field of the Au NHA-based DEP device obtained using FEM: (a) perspective and *x-z* views, (b) electrostatic field intensity (*E*) versus distance (*d*) from the bottom of the Au layer.

Fig. S4: AFM images of the COP film and the fabricated Au NHA.

Fig. S5: Size distribution of the PS NPs measured using dynamic light scattering (DLS).

Fig. S6: SEM images of the trapped PS NPs by DEP after drying the sample dispersion.

Fig. S7: Calibration curve of the PS NPs trapped on the Au NHAs.

Fig. S8: SEM images of the trapped BSA by DEP after drying the sample solution.

Video S1: Fluorescence images obtained during PS NP trapping using the fabricated Au NHA-based DEP device.

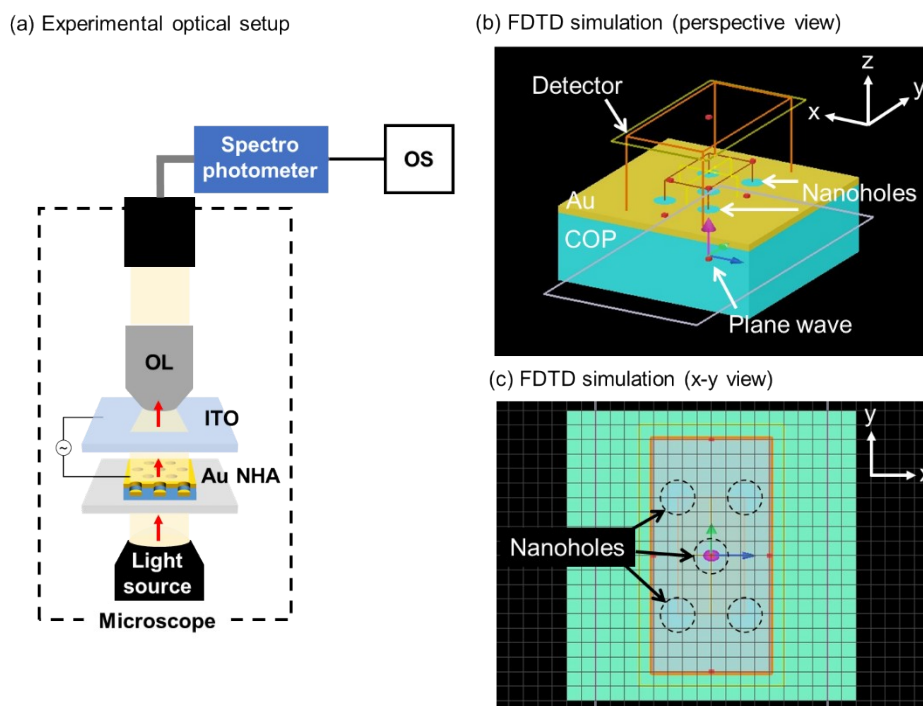


Fig. S1: (a) Schematic of the optical setup used to measure the transmission spectra. (b) and (c) Overview images of the FDTD simulation model of the Au NHA.

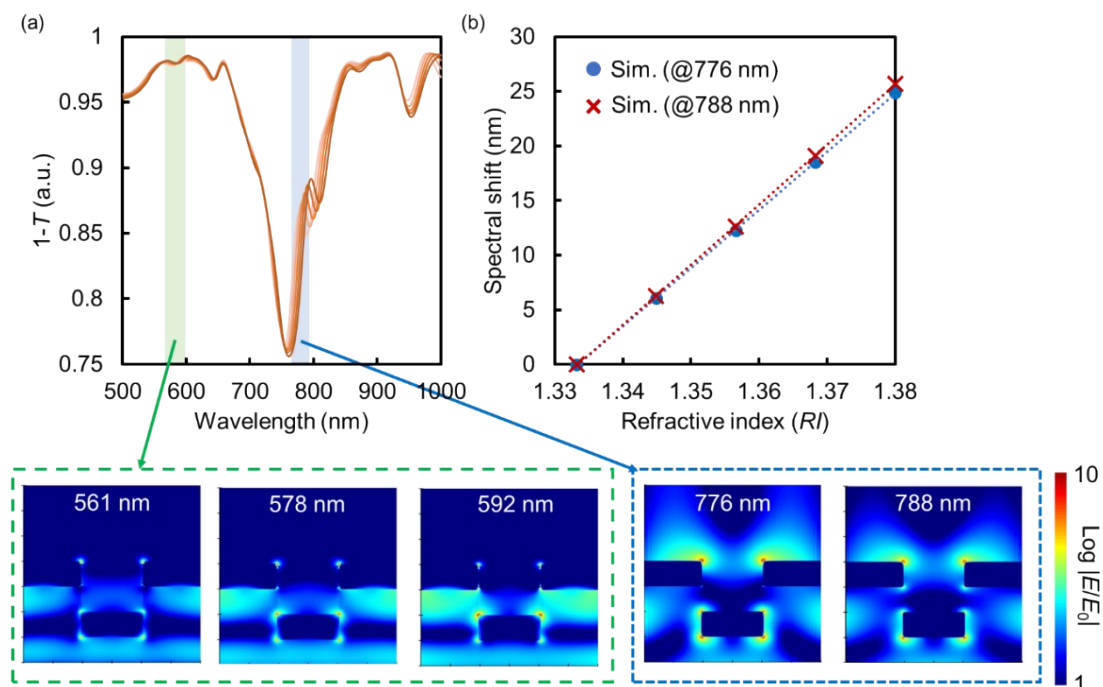


Fig. S2: (a) Absorption spectra with respect to an RI change and EM fields of the Au NHA. (b) Peak and dip shifts with respect to the RI at 776 and 788 nm simulated using the FDTD method. □

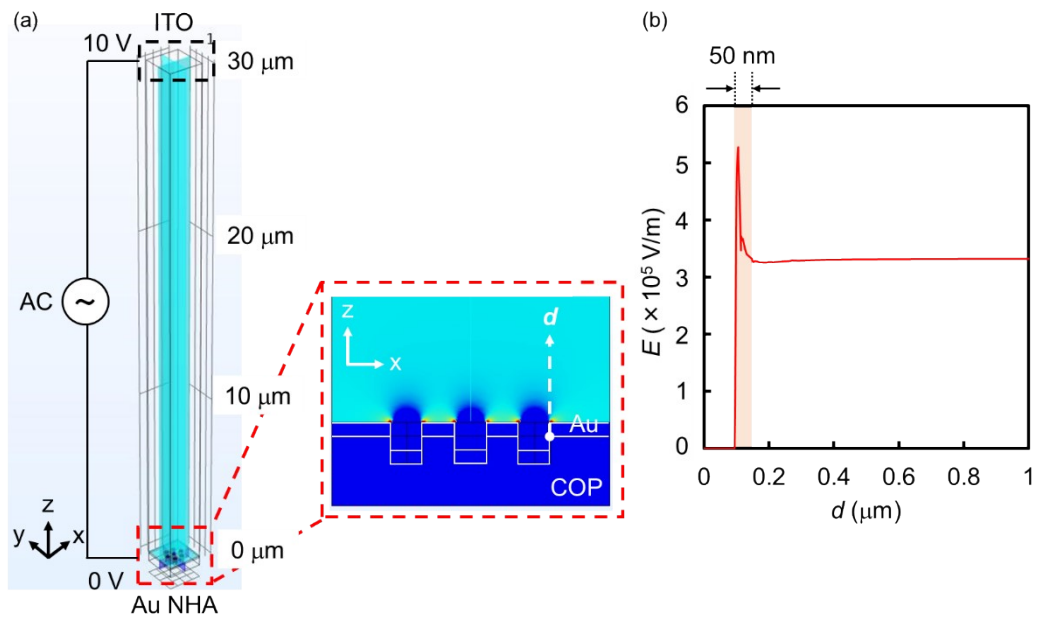


Fig. S3: ES field of the Au NHA-based DEP device obtained using FEM: (a) perspective and x-z views, (b) electrostatic field intensity (E) versus distance (d) from the bottom of the Au layer.

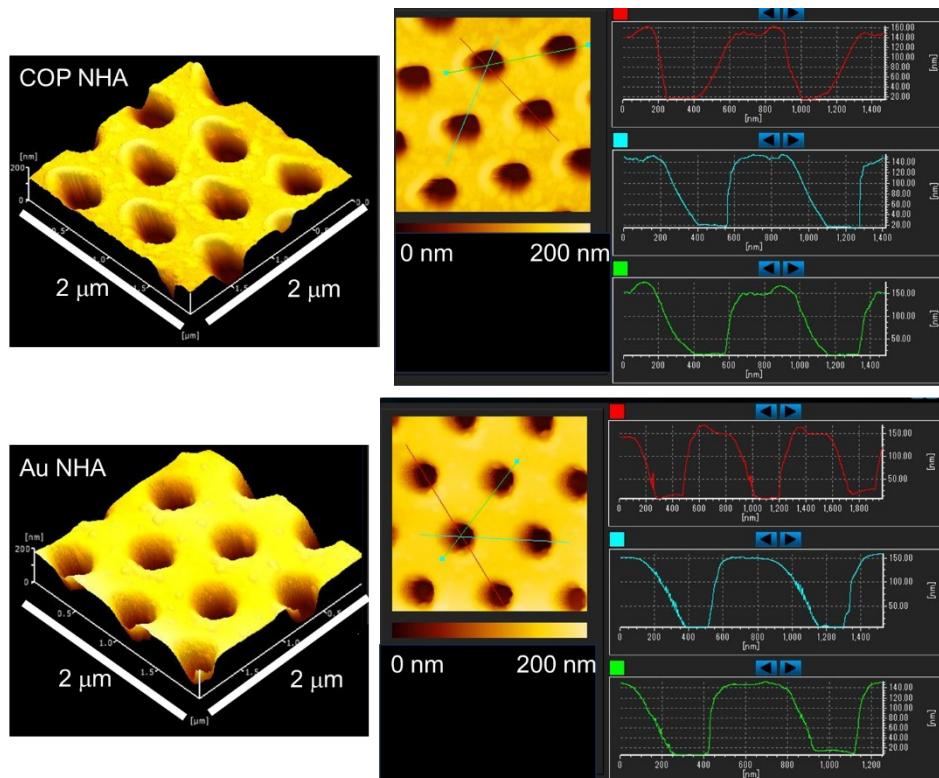


Fig. S4: AFM images of the nanohole-imprinted COP film and the fabricated Au NHA.

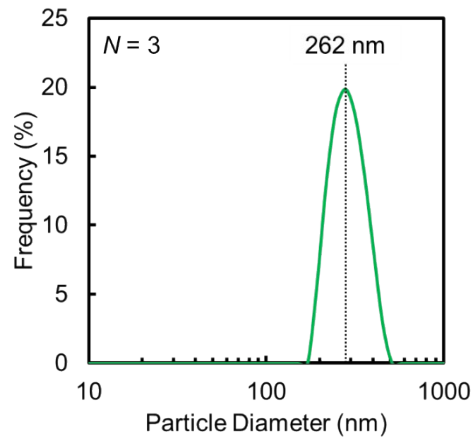


Fig. S5: Size distribution of the PS NPs measured using dynamic light scattering (DLS).

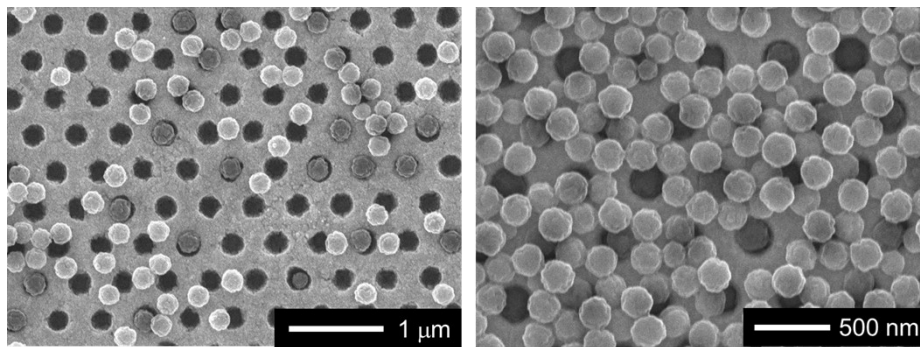


Fig. S6: SEM images of the trapped PS NPs by DEP after drying the sample dispersion.

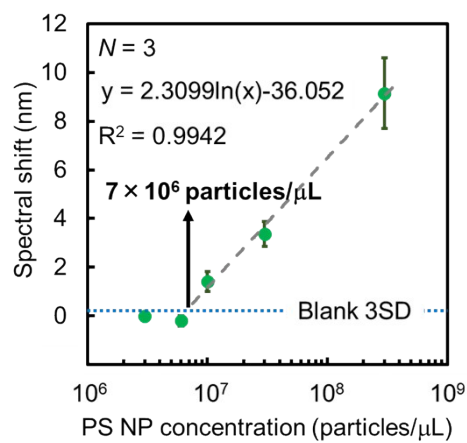


Fig. S7: Calibration curve of the PS NPs trapped on the Au NHAs.

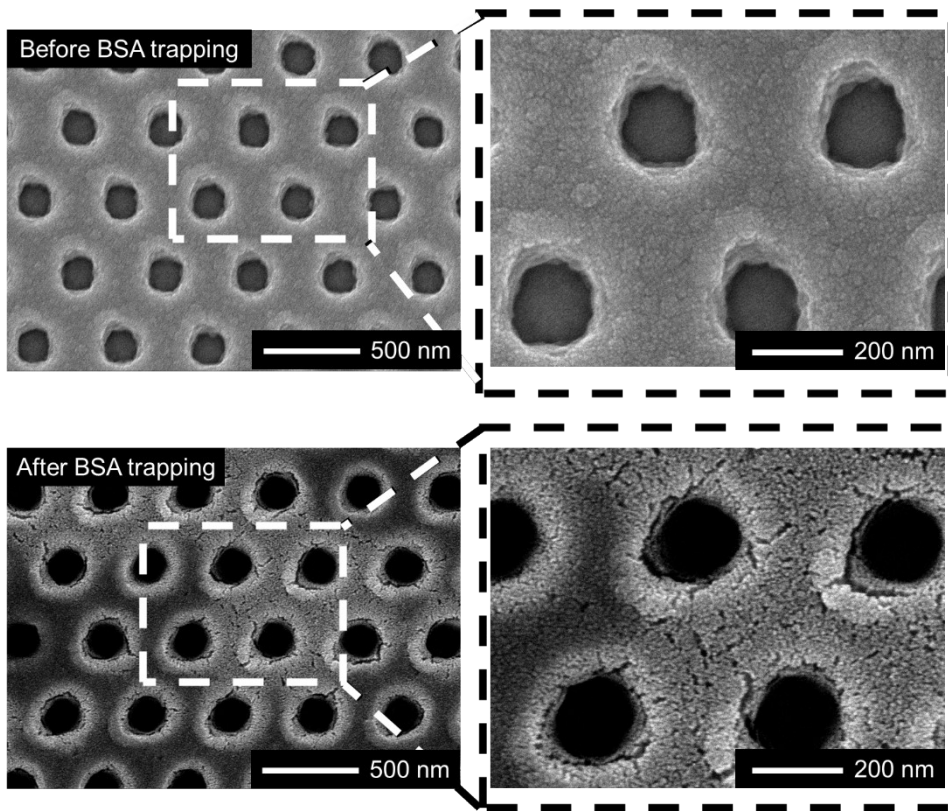


Fig. S8: SEM images of before and after the trapped BSA by DEP after drying the sample solution.